Soft Matter

RSC Publishing

PAPER

View Article Online
View Journal | View Issue

Cite this: *Soft Matter*, 2013, **9**, 1364

Molecularly imprinted conductive polymers for controlled trafficking of neurotransmitters at solid–liquid interfaces†

N. Paul,*[ad] M. Müller,[a] A. Paul,[b] E. Guenther,[c] I. Lauermann,[a] P. Müller-Buschbaum[d] and M. Ch. Lux-Steiner[a]

Received 15th August 2012
Accepted 25th September 2012

DOI: 10.1039/c2sm26896e

www.rsc.org/softmatter

We realize a molecularly imprinted polymer (MIP) which is imprinted with the retinal neurotransmitter glutamate. The films prepared by electrochemical deposition have a smooth surface with a granular morphology as observed using an atomic force microscope. Multiple reflection attenuated total reflection infrared (ATR-FTIR) spectroscopy and X-ray photoelectron spectroscopy (XPS) are used to chemically confirm the imprint of a neurotransmitter in the MIP at the solid–liquid and the solid–air interface, respectively. Fluorescence spectroscopy using the dye fluorescamine is used to monitor the changes in neurotransmitter concentration in various solvents induced by application of voltage to the MIP. By controlling neurotransmitter trafficking across a solid–liquid interface with voltage, we suggest the possibility of using such a neurotransmitter imprinted MIP for chemical stimulation of retinal neurons. The current state of the art approach to restore sight in certain cases of blindness is the replacement of damaged photoreceptors by a subretinal implant consisting of light-sensitive photodiodes. Thus a future perspective of our work would be to chemically stimulate the neurons by replacing the photodiodes in the subretinal implant by the neurotransmitter imprinted polymer film.

I Introduction

Upon entering the eye, light is converted by photoreceptor cells in the retina into electrical impulses which are sent to the brain *via* inter-neuronal communication in the inner retina. The inter-neuronal communication takes places *via* release and binding of neurotransmitters between the pre-synaptic neuron and the post-synaptic neuron. On arrival of nerve impulses, the neurotransmitters are released within milliseconds from the pre-synaptic neuron (*e.g.* photoreceptor cells) into the synaptic cleft (20 nm) where they diffuse in the synaptic fluid until they reach and bind to the postsynaptic membrane receptors. The nerve impulse is then transferred to the post-synaptic neuron. In some incurable diseases of the eye, like retinitis pigmentosa and age-related macular degeneration, the photoreceptor cells are specifically damaged whereas the rest of the visual network remains largely unaffected.[1,2] These diseases lead to loss of vision and presently affect about 15 million people around the world.

There have been many efforts to restore vision by replacing the function of the damaged photoreceptors by artificial retina technology. In the artificial retina device, using the epiretinal approach, a miniature camera mounted in eyeglasses captures images and wirelessly sends the information to a microprocessor (worn on a belt) that converts the data to an electronic signal and transmits it to a receiver on the eye. The receiver sends the signals through a tiny, thin cable to the microelectrode array, stimulating it to emit pulses. The artificial retina device thus bypasses defunct photoreceptor cells and transmits electrical signals directly to the retina's remaining viable cells. The pulses travel to the optic nerve and, ultimately, to the brain, which perceives patterns of light and dark spots corresponding to the electrodes stimulated. Patients learn to interpret these visual patterns.[3–7] While full vision is not restored, the currently used 60 electrodes in Argus II, for example, allow for some distinction of outlines and other basic shapes.[8] The accurate identification of human faces is expected to require approximately a thousand electrodes. The subretinal approach using photocells, led by Zrenner *et al.*, has resulted in restoration of reading in blind test patients.[9–12]

Thus electrical implants are regarded as a feasible way to restore vision in patients suffering from both retinal pigmentosa as well as macular degeneration.[13,14] A common feature in all these approaches is the electrical stimulation of the neurons

[a]*Helmholtz-Zentrum Berlin für Materialien und Energie GmbH, Hahn-Meitner-Platz 1, D-14109 Berlin, Germany*

[b]*Technische Universität München, Physik-Department, LS Neutronenstreuung, James-Franck- Str. 1, 85748 Garching, Germany*

[c]*Natural and Medical Sciences Institute at the University of Tübingen, Markwiesenstr. 55, D-72770 Reutlingen, Germany*

[d]*Technische Universität München, Physik-Department, LS Funktionelle Materialien, James-Franck-Str. 1, 85748 Garching, Germany. E-mail: neelima.paul@ph.tum.de*

† Electronic supplementary information (ESI) available. See DOI: 10.1039/c2sm26896e

of the inner retina. Although this is a viable principle, thousands of pixels are likely to be required for effective restoration of vision for reading. Moreover, the process of electrical stimulation of the downstream neurons is rather unspecific. In the approximate environment of the electrode all signal paths and cell types are stimulated. Additionally, the switching by electrical impulses may cause long term damage for the tissue.

Alternative investigations to the electrical approach have been performed; for example, micro-contact printing to direct cultured retinal ganglion cell neurites to precise stimulation positions.[15] Other groups have demonstrated the feasibility of using organic electronics with conductive polymers (like PEDOT) for electronic control of Ca^{2+} signalling in neuronal cells and using neurotransmitters for directly modulating mammalian sensory function.[16,17] Recently, we proposed the possibility of yet another alternative to the electric stimulation of the downstream neurons, which is a biochemistry based retinal implant using the retinal neurotransmitter, glutamate.[18] The principle of our envisaged device is comparable to the natural release process of neurotransmitters in the retina where the glutamate is continuously released from photoreceptors in the dark and the release is stopped when light falls on the retina. The aim is the replacement of the photoreceptor function after degeneration by a neurotransmitter imprinted polymer (n-MIP) implant. The activity of the subsequent neuron (the bipolar, horizontal) would be modulated by the messenger molecules (glutamate) which will be bound to or released from the n-MIP implant from or to the surrounding liquid environment dependent on the light situation.

The proposed implant is comprised of a glutamate-doped-polypyrrole film (also referred to as n-MIP throughout this manuscript), electrochemically deposited on a conductive electrode, such as silicon or gold. By changing the electrode potential, using an external power supply, we explored if the n-MIP film can reversibly bind/release the neurotransmitter, glutamate, from/into the surrounding solvent.

The use of polymers in biomedical applications is well studied.[19–26] Polypyrrole (PPy) is an electrically conductive polymer and is well known in the area of chemical sensors[27,28] and different approaches have been used to achieve polypyrrole nanostructures.[29] Its application as molecular recognition elements in molecularly imprinted polymer (MIP) systems has just recently emerged.[30–35] It can be used in a neutral pH region, and stable films can conveniently be polymerized on various substrates. In contrast to its monomer pyrrole, PPy is biocompatible and biological cells can grow on it.[36] Molecularly imprinted polymers are synthesized in the presence of a template molecule which is identical to the target molecule that the polymer should later selectively bind. Therefore, the straightforward analogy between MIPs and biological receptors accounts for possible applications relying on specific molecular binding events.[37,38]

Glutamate is an amino acid and more than half of the nervous system utilizes it as a neurotransmitter. Its chemical structure varies from acidic (NH_2RCOOH), to anionic (NH_2RCOO^-), to cationic (NH_3^+RCOOH), or to zwitterionic ($NH_3^+RCOO^-$), according to their environmental pH.[39] In the pH interval from 4.3 to 9.7, which is most important for biological processes, glutamate exists in the zwitterionic form. This attributes to glutamate, a net negative charge (two negative charges from the two deprotonated carboxylates and one positive charge from the protonated amine group). We use this charge to electrostatically bind/release glutamate from charging surfaces like MIPs which can be made specific to glutamate by using it as the template molecule.

II Materials and methods

All chemicals were purchased from Sigma Aldrich. A fresh stock of 3 mg ml^{-1} fluorescamine was prepared by dissolving the required quantity in acetone. Fluorescamine is a non-fluorescent compound (dye) which reacts rapidly with primary amines in amino acids and peptides to form highly fluorescent moieties.[41] When activated with the UV light source (365 nm), the fluorescence of the protein–dye complex has an emission wavelength of approximately 470 nm. All experimental solutions obtained from the electrochemical cell were examined after thoroughly mixing them with equal quantities of the fluorescamine stock solution. The fluorescence was measured using a fluorescence spectrometer (Perkin Elmer LS50B) after waiting 45 minutes for stabilization of the final solution. The excitation wavelength of this instrument was fixed at 365 nm and the emission was measured in the region of 440 nm to 500 nm.

In this paper, we have chosen PPy as the polymer to be molecularly imprinted with the neurotransmitter glutamate. To prepare the glutamate-doped-PPy, a three-electrode electrochemical cell (made of glass) was used in combination with a potentiostat. A clean platinum wire was used as the counter electrode and an Ag/AgCl electrode was used as the reference electrode. The Si working electrode had been cleaned using piranha solution and HF (hydrofluoric acid) etching, whereas the Au working electrode had been cleaned by several cycles of cyclic voltammetry in 0.1 M sulphuric acid electrolyte solution. Before starting the deposition, pyrrole was vacuum-distilled and the electrolyte solution, consisting of 0.4 M pyrrole and 0.5 M glutamate, was flushed with nitrogen gas. PPy was then electrochemically deposited on the working electrode from the electrolyte solution. During electrodeposition, the working electrode was maintained at a constant voltage of 0.6 V for 30 minutes. Subsequently, the PPy films were overoxidised in a phosphate buffered saline solution with a pH of 7.4. To achieve overoxidation, a constant current of 0.025 mA was applied to the working electrode until a potential of 1.4 V was reached. To prepare the chlorine-doped-PPy (the control polymer film which is imprinted with chlorine instead of glutamate), glutamate was replaced by chlorine in the electrolyte solution.

The phosphate buffered saline solution was prepared by dissolving together 137 mM NaCl, 2.7 mM KCl, 10 mM $Na_2HPO_4 \cdot 2H_2O$, and 2 mM KH_2PO_4 in a solution to get pH 7.4. The Ringer's solution was prepared by dissolving 147 mM NaCl, 4 mM KCl, and 2.2 mM $CaCl_2$ in another aqueous solution.

Atomic force microscopy (AFM) measurements were done to study the surface morphology of samples in air using the instrument Park Systems XE-70 in the non-contact mode.

X-ray photoemission spectra were obtained at the Helmholtz Zentrum Berlin using a custom-made UHV system equipped with a CLAM 4 hemispherical electron energy analyzer and a SPECS XR 50 X-ray gun using Mg K radiation. The energy calibration was performed by measuring the Au $4f_{7/2}$ peak from a clean Au/glass substrate and assuming a binding energy of 84.0 eV.[42] The fitting was performed using Peakfit software (Hearne Scientific Software Ltd., Australia) and Voigt functions were applied to determine the individual peaks.

For the Fourier Transform Infrared (FTIR) spectroscopy, a commercial FTIR device 113v (Bruker GmbH, Germany) equipped with an attenuated total reflection (ATR) unit was used. The resolution of the IR spectra was 4 cm^{-1}. The signal/noise ratio of an FTIR spectrum was increased by averaging 1024 scans using a photovoltaic mercury cadmium telluride infrared detector. The optically polished Si ATR crystal had the dimension ($2 \times 45^{\circ}$, 50 ± 0.2 mm $\times$ 10 ± 0.1 mm $\times$ 3 mm). The ATR geometry allows for multiple reflections which provide an enhanced sensitivity to chemical identification of molecular species at the solid–liquid interface. It provides an IR sensitivity of the order of 10% of an adsorbate monolayer and the possibility of monitoring species that absorb in the water absorption range.[43]

III Results and discussion

Fig. 1 shows a schematic of the envisaged implant site and the proposed idea. Our intention is to regulate the glutamate concentration in the liquid with voltage applied to the glutamate-doped-molecularly imprinted polymer (also referred to as n-MIP). In the rest state, when there is no voltage, there is an initial concentration of glutamate (few mM) in the liquid. By application of a positive voltage to the n-MIP, the glutamate molecules are attracted to the n-MIP and adsorbed on the n-MIP from the liquid, thereby leading to a decrease in the glutamate concentration in the liquid. On removal of the voltage, the glutamate is released back into the liquid, leading to an increase in the glutamate concentration in the liquid. This process is expected to be reversible. The advantage would be the direct control of this uptake and release of neurotransmitters and therefore a specific access to the successional neurons. In this work, we demonstrate the proof of principle of this device by verifying the change in the concentration of glutamate with voltage in physiological solvents (such as Ringer solution containing glutamate). The replenishment of the template depleted polymer is planned by an addition of glutamate reservoirs in the vicinity of the implant site which will very slowly release a controlled amount of glutamate into the synapse. Such a reservoir system has already been demonstrated to contain sufficient glutamate so that refills of the reservoir are seldom necessary.[44] Another future step and also beyond the scope of this article would be testing the activation of retinal cells by placing an isolated retina on a flat n-MIP device and then recording the response of the retinal ganglion cells with an extracellular electrode.

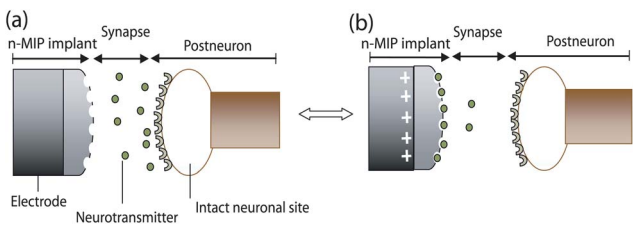

Fig. 1 Schematic diagram of the synaptic cleft and the proposed implant at the preneuron (photoreceptor) site showing (a) the rest state (without voltage stimulation) corresponding to an initial concentration (or release state) of the neurotransmitter in the synapse and (b) the active state (with voltage stimulation) corresponding to binding of the neurotransmitter to the n-MIP.

A Surface morphology

The morphology of the glutamate-doped-PPy film on Si was examined using an AFM. The film surface is smooth and consists of homogeneously distributed and spherically shaped grains as shown in Fig. 2b. The line scans indicate that these granular structures have an average diameter of about 100 nm and an average height of about 5 nm in a region of 0.5 $\times$ 0.5 μm^2. The height/width in the image is $\sim$0.05 and these are reasonable dimensions for a possible implant material.

B Imprint of a neurotransmitter in the polymer film

Using FTIR spectroscopy, the presence of glutamate within a polymer (like PPy) can be confirmed by detecting the vibration characteristics of the specific functional groups in its chemical structure. Lanzilotta and McQuillan[39] had studied the aqueous solution spectra of glutamic acid using single reflection ATR infrared spectroscopy and identified most of the functional groups. At pH 6, they assigned glutamate by the characteristic stretching vibrations at 1400 cm^{-1}, 1556 cm^{-1} and 1593 cm^{-1}. In our studies we used multiple reflection ATR-FTIR spectroscopy to enhance the signal from the solid–solution interface and reduce the signal from the solution. Moreover, water (H_2O) was replaced by heavy water (D_2O) for separating the water bands which also lie in the similar region as the peaks of glutamate and PPy.

The absorption peaks of glutamate on a Si ATR crystal occur at 1400 cm^{-1}, 1565 cm^{-1} and 1610 cm^{-1} as shown in the inset of Fig. 3. The peaks at 1400 cm^{-1} and 1565 cm^{-1} are attributed to the symmetric and asymmetric stretching of the carboxylate groups and the peak at 1610 cm^{-1} is due to a combination of the vibrations of the amine group and the carbonyl group which has been downshifted due to strong lateral bonds between the glutamate monolayer.

For comparison, we first discuss the infrared spectrum of chlorine-doped-PPy in Fig. 3a, which is a 'control polymer film' for our studies. It contains chlorine instead of glutamate as the dopant molecule. The peak at 1535 cm^{-1} is due to the asymmetric stretching mode of the pyrrole ring. The absorption at 1580 cm^{-1} can be assigned to the C=C ring stretching of pyrrole. It is down-shifted from the normally observed 1630 cm^{-1} position[40] due to the present spectrum being taken in heavy water. The infrared spectrum of glutamate-doped-PPy film is shown in Fig. 3b. The absorption peaks of glutamate, normally observed at 1565 cm^{-1} and 1610 cm^{-1}, are shifted

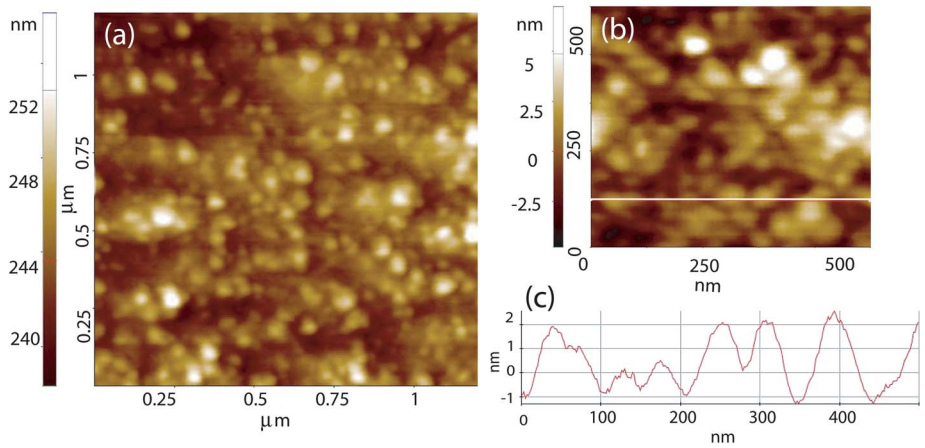

Fig. 2 (a) A two-dimensional AFM image of a glutamate-doped molecularly imprinted polymer and (b) a magnified region of the same film showing grains having an average diameter of 100 nm and an average height of 5 nm (c) The line scans across the surface of the polymer show a relatively smooth and homogeneous granular (height/width in the image ~0.05) film.

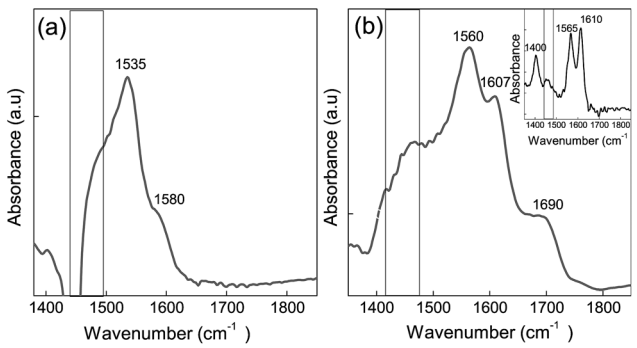

Fig. 3 (a) ATR-FTIR difference spectrum of chlorine-doped-PPy (control PPy film without glutamate imprint) film on a Si crystal/D_2O solution. (b) ATR-FTIR difference spectrum of glutamate-doped-PPy film on a Si crystal/D_2O solution. There is no glutamate in the solution. The background spectrum was a clean Si crystal/D_2O solution. Inset shows the IR spectrum of pure glutamate/D_2O solution. The rectangle corresponds to a region of the adsorption edge of Si which causes noise in the spectrum.

slightly to lower frequencies due to accommodation of glutamate within the polypyrrole matrix. The peak at 1400 cm^{-1} has also decreased in intensity due to a reduced contribution from the symmetric stretching contribution of at least one of the carboxylate groups due to its conversion into a carbonyl group. This conversion can be confirmed by the observance of a band at 1690 cm^{-1} which is also downshifted in frequency from 1720 cm^{-1} (as expected from the carbonyl group of an unbound glutamate). The spectra not only identify glutamate in the n-MIP but also indicate that glutamate is adsorbed in a state where at least one of the two carboxylate groups is converted into a carbonyl group. We would like to emphasize here that there was no glutamate in the D_2O solution. Thus the observed signal is from the glutamate embedded in the PPy itself.

X-ray photoelectron spectroscopy measurements were carried out to provide information on the chemical and electronic structure of glutamate-doped-PPy films. Measurements on chlorine-doped-polypyrrole films (the 'control polymer film') were also done for comparison. The C 1s and N 1s spectra of both films are shown in Fig. 4a–d. The main peak in the C 1s photoemission of chlorine-doped-PPy films, in Fig. 4a, is centered at about 285.2 eV. It is due to the C–C bonds due to the aromatic carbons of the pyrrole rings of PPy[45] whose photoemission is slightly shifted to larger energies due to interaction with the anions. We also observe that the carbon peak is asymmetric and skewed toward the high binding energy site.

On the other hand, in Fig. 4b, the C 1s spectra of glutamate-doped-PPy films clearly indicates the existence of two inequivalent carbon atoms with photoemissions at 285.5 eV and 289 eV. The chemical splitting of the C 1s peak indicates a specific site electrostatic interaction *i.e.*, the presence of bipolarons. The main peak at 285.5 eV is due to C–C bonds of pyrrole rings and it is slightly shifted towards higher energy due to electrostatic interaction with glutamate anions. The second peak which is chemically shifted by 3.5 eV is due to carboxylate groups of the glutamate anion.

In Fig. 4c, the N 1s photoemission of the chlorine-doped-PPy film results in a major peak centered at about 400 eV. It is attributed to nitrogen atoms of pyrrole that are least affected by the presence of the anions.[46] The shoulder peak at 401.5 eV is due to the nitrogen atoms which are electrostatically attracted to the anions.[48,49] The complete transfer of a unit charge from dopant anion to the nitrogen of the pyrrole ring would have resulted in a binding energy shift of 5.8 eV of the shoulder peak from the major peak.[48,49] The observed shift of only 1.5 eV implies that only a charge of 1/4 e is transferred to the nitrogen while the rest is distributed among the 4 carbons of the pyrrole unit. Thus the anion charge is uniformly distributed over all the 5 atoms of the pyrrole ring.

The line shape analysis of the N 1s spectra of glutamate-doped-PPy films in Fig. 4d clearly indicates the existence of three peaks. The peak at 402.2 eV which is shifted by about 2.2 eV from the main nitrogen feature is most likely due to the photoemission from the protonated amino groups of the glutamate anion.[47,50] Thus, the XPS analysis of the doped PPy films indicates that the electrostatic interaction with the dopant

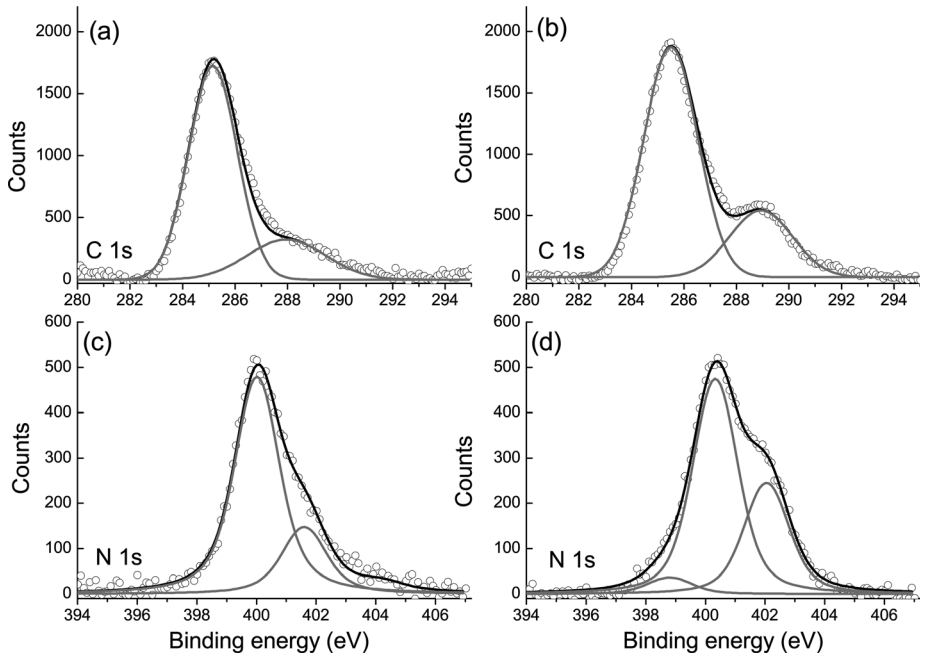

Fig. 4 (a and b) C 1s X-ray photoelectron spectra of the chlorine-doped-PPy (control PPy film without glutamate imprint) and glutamate-doped-PPy films respectively. (c and d) N 1s X-ray photoelectron spectra of the chlorine-doped-PPy and glutamate-doped-PPy films respectively.

anions is not only restricted to the nitrogen atoms and that the carbon atoms of the pyrrole ring are also involved. Moreover, we also chemically identify glutamate in the glutamate-doped-PPy film due to the photoemission from its carboxylate groups in the C 1s spectra and the photoemission from its protonated amino groups (NH_3^+) in the N 1s spectra.

C Changes in neurotransmitter concentration

Fluorescence based methods offer the possibility to measure properties and interactions of protein with a high sensitivity and selectivity.[51,52] Thus, one way to investigate the adsorption/release of biomolecules at the solid–liquid interface is to monitor the concentration of biomolecules in the liquid using fluorescence spectroscopy. In this technique, a fluorescent dye (which by itself does not have any fluorescence, *e.g.* fluorescamine) is added to the liquid under investigation, and the resulting fluorescence intensity (due to binding of the dye to the biomolecule) corresponds to the amount of biomolecules in the liquid. We obtained a calibration curve between fluorescence intensity and concentration of glutamate by monitoring the fluorescence at 470 nm for fluorescamine solutions, each containing different concentrations of glutamate. As can be seen in Fig. 5 we find a linear relationship between fluorescence and concentration and thus the Beer–Lambert law can be applied. A calibration factor of 2.7 (intensity unit/μM) was determined.

Fig. 6 shows the set-up of the experimental cell used to determine the change in concentration of glutamate in a solvent with application of voltages to the glutamate-doped-PPy electrode. In each experimental series the electrochemical cell contained 5 mM glutamate dissolved in different solvents (*e.g.* water, phosphate buffer saline or Ringer solution). The buffer and Ringer aqueous solutions not only offer the physiological pH 7.4 but also contain several other ions which are in competition with glutamate in the voltage induced binding/release process. The solvents were continuously stirred during the experiment. Voltage steps, each of three minutes duration, were applied to the n-MIP film by an external power supply. During that time, a very small amount of the solution was extracted for analysis by fluorescence spectroscopy. This particular initial concentration of 5 mM glutamate was used so that only a minute amount of test solution needs to be taken out of the electrochemical cell during in-situ voltage application and a later dilution step would ensure that the minimum required quantity of test solutions for fluorescence analysis was obtained. This concentration of glutamate is about 50 times higher than the concentration of glutamate in the extracellular solution within the synaptic cleft. The glutamate molecules present in the extracted sample solution were all diluted by a

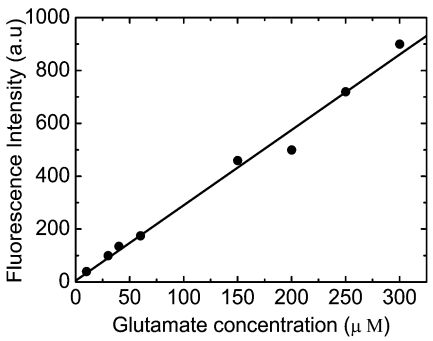

Fig. 5 Calibration curve showing a linear relation between the fluorescence intensity and glutamate concentration in the liquid. Each point represents the average of three identical experiments.

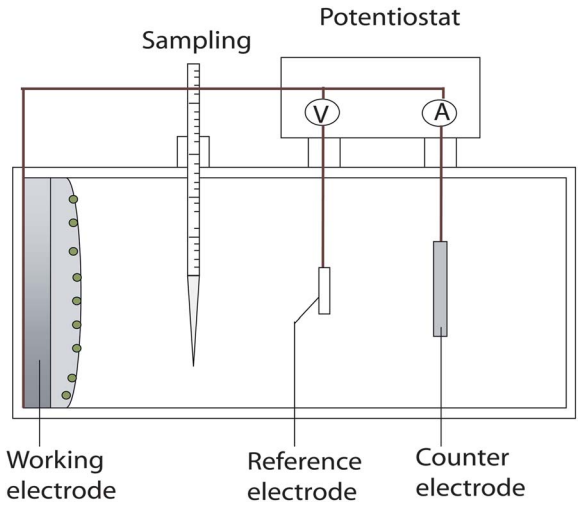

Fig. 6 A schematic of the electrochemical cell from which the liquid samples for fluorescence analysis were extracted.

factor of 1/50 (to get them in the range of the calibration curve and in order of actual glutamate concentration in physiological solutions) and labelled with fluorescamine.

After a stabilization time of 45 minutes, the fluorescence intensities were noted. The intensity of the emitted fluorescence radiation quantifies the amount of glutamate molecules and accordingly their concentration. The glutamate concentrations are calculated from the fluorescence intensities by dividing the observed intensities with the calibration factor and compensating for the dilution factor. The dependence of glutamate concentration in the solvents on the application of voltage pulses on the n-MIP electrode is shown in Fig. 7.

For all three solutions, the trend is similar. For positive voltages the glutamate concentration decreases which can be interpreted as binding of the negatively charged glutamate molecules to the positively charged n-MIP electrode, thereby leading to a decrease in the number of glutamate molecules in the solvent. At negative voltages, glutamate molecules experience an electrostatic repulsion from the negatively charged n-MIP film and thus an increase (or recovery to initial concentration) in the number of glutamate molecules in the solvent occurs. In Fig. 7(b) and (c) one can see that even when glutamate is dissolved in solvents containing a mixture of other ions, such as phosphate buffer saline solution (containing ions such as Na^+, Cl^-, K^+ and PO_4^-) and Ringer solution (containing Na^+, Ca^+, Cl^-, and K^+) solutions, the glutamate-doped-PPy surface is still selective for glutamate. Such behavior is expected as it is well known from literature on molecularly imprinted polymers that a molecularly imprinted polymer, which is doped with a specific dopant molecule during polymerization, will only be able to modulate the uptake-release of that specific molecule. In our case, the specific dopant molecule is glutamate for the n-MIP film. Moreover, for all investigated solutions, the process seems completely reversible.

As a control measurement, we replaced the n-MIP electrode by two different control electrodes which are both not imprinted with glutamate. The control electrodes are Cl-doped-PPy

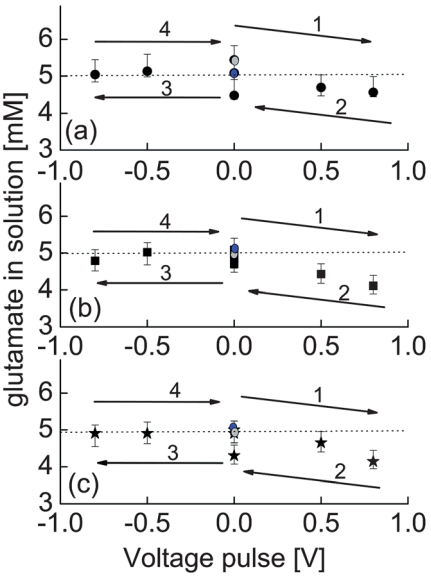

Fig. 7 Changes in glutamate concentration calculated from the fluorescence intensities as a result of voltages applied to the glutamate-doped-PPy film surface in (a) water, (b) phosphate buffer saline solution, and (c) Ringer's solution. The blue circle indicates the initial concentration and the grey circle denotes the final concentration at the end of the cycle. The arrows define the sequence of the process.

and spin coated PPy, on which we have repeated the process of voltage application and fluorescence estimation. In Fig. 8 it can be seen that although these non-imprinted electrodes also initially show some decrease in glutamate concentration at positive voltages, it is within error and the decrease is not maintained at higher positive voltages. Moreover, they do not permit the complete recovery of the glutamate concentration in

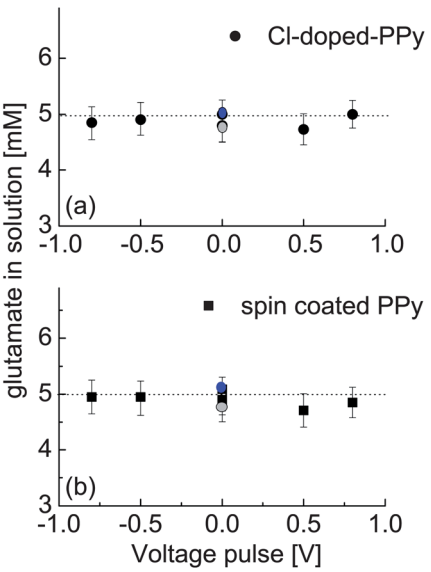

Fig. 8 Changes in glutamate concentration in phosphate buffer saline solutions, calculated from the fluorescence intensities, as a result of voltages applied to (a) Cl-doped-PPy and (b) spin coated PPy electrodes. The blue circle indicates the initial concentration and the grey circle denotes the final concentration at the end of the cycle.

the solution at the end of the cycle. This is due to the non-specific (and chemical) binding of glutamate to the control electrodes. In the case of the imprinted polymer, the change in glutamate concentration is seen in a controlled manner and a complete recovery of the glutamate concentration to its initial value is possible which also points to the replenishment of the polymer during the voltage cycle.

In some very recent work a similar process has been studied using a combination of electrochemistry and quartz crystal microbalance. With application of voltage, it was possible to control the mass/frequency changes on a solid–liquid (imprinted polymer/buffer solution) interface.[36] With quartz crystal microbalance, however, a chemical identification of the species which causes the mass change is not possible. In contrast, our work demonstrates the chemical evidence that it is the glutamate's concentration which is being changed. Thus our studies using fluorescence spectroscopy chemically and quantitatively identify reversible and controlled changes in glutamate concentration in solutions, also in competition with other ions, where a complete recovery to initial concentration is also possible.

IV Conclusion

A neurotransmitter-doped-molecularly imprinted polymer is proposed that can, as a reaction to the applied voltage, reversibly attract/repel glutamate molecules from/to the surrounding solvents. Fluorescence spectroscopy studies using the dye fluorescamine have succeeded in showing a reversible concentration change of 1 mM in glutamate in physiological solvents. Atomic force microscopy reveals a smooth surface and a uniform granular morphology of the electrochemically prepared polymer film. Infrared spectroscopy and X-ray photoelectron spectroscopy confirm chemically the imprint of a neurotransmitter in the polymer film at solid–liquid and solid–air interfaces respectively.

This work suggests a novel idea of developing a neurotransmitter based retinal prosthesis. Presently, it is realized with the help of an external power supply. A future perspective would be to replace the substrate by a solar cell and test the device on actual retinal cells. In this way, the incident light could induce a photovoltage and thereafter govern the binding/release of glutamate directly. Thin, conducting PPy films are largely transparent to visible light.[53] Accordingly, the study of PPy films grown on silicon and the interaction dynamics between glutamate and the PPy is a consequential step towards this direction.

Acknowledgements

This work was supported by Bundesministerium für Bildung und Forschung Rahmenprogramm Mikrosystemtechnik. We would like to thank Claudia Zielke for technical assistance in measuring the XPS spectra.

References

1 N. Congdon, *et al.*, Causes and prevalence of visual impairment among adults in the United States, *Arch. Ophthalmol.*, 2004, **122**, 477–485.
2 B. W. Jones and R. E. Marc, Retinal remodeling during retinal degeneration, *Exp. Eye Res.*, 2005, **81**, 123–137.
3 J. D. Weiland, W. Liu and M. S. Humayun, Retinal prosthesis, *Annu. Rev. Biomed. Eng.*, 2005, **7**, 361–401.
4 D. Yanai, *et al.*, Visual Performance using a retinal prosthesis in three subjects with retinitis pigmentosa, *Am. J. Ophthalmol.*, 2007, **143**(5), 820–827.
5 A. K. Ahuja, M. R. Behrend, M. Kuroda, M. S. Humayun and J. D. Weiland, An *in vitro* Model of a retinal prosthesis, *IEEE Trans. Biomed. Eng.*, 2008, **55**(6), 1744–1753.
6 A. Caspi, *et al.*, Feasibility study of a retinal prosthesis: spatial vision with a 16-electrode implant, *Arch. Ophthalmol.*, 2009, **127**(4), 398–401.
7 D. Palanker, A. Vankov, P. Huie and S. Baccus, Design of a high resolution Optoelectronic retinal prosthesis, *J. Neural Eng.*, 2005, **2**, S105–S120.
8 J. D. Weiland, A. K. Cho and M. S. Humayun, Retinal prostheses: current clinical results and future needs, *Ophthalmology*, 2011, **118**, 2227–2237.
9 E. Zrenner, Will retinal implants restore vision?, *Science*, 2002, **295**, 1022–1025.
10 E. Zrenner, *et al.*, Subretinal electronic chips allow blind patients to read letters and combine them to words, *Proc. Biol. Sci.*, 2011, **278**(1711), 1489–1497.
11 E. Guenther, B. Troeger, B. Schlosshauer and E. Zrenner, Long-term survival of retinal cell cultures on retinal implant materials, *Vis. Res.*, 1999, **39**, 3988–3994.
12 E. Zrenner, *et al.*, Can subretinal microphotodiodes successfully replace degenerated photoreceptors?, *Vis. Res.*, 1999, **39**, 2555–2567.
13 N. B. Dommel, Y. T. Wong, T. Lehmann, N. H. Lovell and G. J. Suaning, A CMOS retinal neurostimulator capable of focussed, simultaneous stimulation, *J. Neural Eng.*, 2009, **6**, 035006–035016.
14 D. Yanai, J. D. Weiland, M. Mahadevappa, R. J. Greenberg, I. Fine and M. S. Humayun, Visual performance using a retinal prosthesis in three subjects with retinitis pigmentosa, *Am. J. Ophthalmol.*, 2007, **143**, 820–827.
15 T. Leng, P. Wu, N. Z. Mehenti, S. F. Bent, M. F. Marmor, M. S. Blumenkranz and H. A. Fishman, *Invest. Ophthalmol. Visual Sci.*, 2004, **45**, 4132.
16 J. Isaksson, *et al.*, Electronic control of Ca^{2+} signalling in neuronal cells using an organic electronic ion pump, *Nat. Mater.*, 2007, **6**, 673–679.
17 D. T. Simon, *et al.*, Organic electronics for precise delivery of neurotransmitters to modulate mammalian sensory function, *Nat. Mater.*, 2009, **8**, 742–746.
18 Patent application 'Implantierbares System zur Anregung von Neuronen', Document identification DE102007020 305A1, 23.10.2008.
19 M. Schulz, A. Olubummo and W. H. Binder, Beyond the lipid-bilayer: interaction of polymers and nanoparticles with membranes, *Soft Matter*, 2012, **8**, 4849–4864.
20 M. Welch, A. Rastogi and C. Ober, Polymer brushes for electrochemical biosensors, *Soft Matter*, 2011, **7**, 297–302.
21 H. Sun, *et al.*, Amino acid containing degradable polymers as functional biomaterials: rational design, synthetic pathway,

and biomedical applications, *Biomacromolecules*, 2011, **6**, 1937–1955.
22 J. C. Cuggino, *et al.*, Thermosensitive nanogels based on dendritic polyglycerol and *N*-isopropylacrylamide for biomedical applications, *Soft Matter*, 2011, **7**, 11259–11266.
23 F. Li, *et al.*, Thermally sensitive dual fluorescent polymeric micelles for probing cell properties, *Soft Matter*, 2011, **7**, 11211–11215.
24 F. Meng, Z. Zhong and J. Feijen, Stimuli-responsive polymersomes for programmed drug delivery, *Biomacromolecules*, 2009, **10**(2), 197–209.
25 V. Kozlovskaya, J. F. Ankner, H. O'Neill, Q. Zhang and E. Kharlampieva, Localized entrapment of green fluorescent protein within nanostructured polymer films, *Soft Matter*, 2011, **7**, 11453–11463.
26 G. G. Wallace, S. E. Moulton and G. M. Clark, *Science*, 2009, **324**, 185–186.
27 J. Janata and M. Josowicz, Conducting polymers in electronic chemical sensors, *Nat. Mater.*, 2003, **2**, 19–24.
28 V. S. Ijeri, *et al.*, An elegant and facile single-step UV-curing approach to surface nano-silvering of polymer composites, *Soft Matter*, 2010, **6**, 4666–4668.
29 M. A. Ruderer, M. Hirzinger and P. Müller-Buschbaum, Photoactive nanostructures of polypyrrole, *ChemPhysChem*, 2009, **10**, 2692–2697.
30 L. D. Spurlock, A. Jaramillo, A. Praserthdam, J. Lewis and A. Brajter-Toth, Selectivity and sensitivity of ultrathin purine-templated overoxidized polypyrrole film electrodes, *Anal. Chim. Acta*, 1996, **336**, 37–46.
31 B. Deore, Z. D. Chen and T. Nagaoka, Potential-induced enantioselective uptake of amino acid into molecularly imprinted overoxidized polypyrrole, *Anal. Chem.*, 2000, **72**, 3989–3994.
32 X. Lui, K. J. Gilmore, S. E. Moulton and G. G. Wallace, *J. Neural Eng.*, 2009, **6**, 065002.
33 A. Gelmi, M. J. Higgins and G. G. Wallace, *Biomaterials*, 2010, **8**, 1974–1983.
34 V. Syritski, J. Reut, A. Menaker, R. E. Gyurcsinyi and A. Opik, *Electrochim. Acta*, 2008, **53**, 2729–2736.
35 Y. Kong, W. Zhao, S. Yao, J. Yu, W. Wang and Z. Chen, *J. Appl. Polym. Sci.*, 2010, **115**, 1952–1957.
36 E. von Hauff, K. Fuchs, D. Ch. Hellmann, J. Parisi, R. Weiler, C. Burkhardt, U. Kraushaar and E. Guenther, Biocompatible molecularly imprinted polymers for the voltage regulated uptake and release of L-glutamate in neutral pH solutions, *Biosens. Bioelectron.*, 2010, **26**, 596–601.
37 K. Haupt, Imprinted polymers - tailor-made mimics of antibodies and receptors, *Chem. Commun.*, 2003, **2**, 171–178.
38 K. Mosbach, Molecular imprinting, *Trends Biochem. Sci.*, 1994, **19**, 9–14.
39 A. D. Roddick-Lanzilotta and A. J. McQuillan, An *in situ* infrared spectroscopic study of glutamic acid and of aspartic acid adsorbed on TiO_2: implications for the biocompatibility of titanium, *J. Colloid Interface Sci.*, 2000, **227**, 48–54.
40 H. Kato, O. Nishikawa, T. Matsui, S. Honma and H. Kokado, Fourier transform infrared spectroscopy study of conducting polymer polypyrrole: higher order structure of electrochemically-synthesized film, *J. Phys. Chem.*, 1991, **95**(15), 6014–6016.
41 S. Udenfriend, S. Stein, P. Boehlen, W. Dairman, W. Leimgruber and M. Weigele, Fluorescamine: a reagent for assay of amino acids, peptides, proteins, and primary amines in the picomole range, *Science*, 1972, **178**, 871–872.
42 A. Vollmer, O. D. Jurchescu, I. Arfaoui, I. Salzmann, T. T. M. Palstra, P. Rudolf, J. Niemax, J. Pflaum, J. P. Rabe and N. Koch, The effect of oxygen exposure on pentacene electronic structure, *Eur. Phys. J. E*, 2005, **17**, 339–343.
43 J. N. Chazalviel, B. H. Erne, F. Maroun and F. Ozanam, *In situ* infraredspectroscopy of the semiconductor vertical bar electrolyte interface, *J. Electroanal. Chem.*, 2001, **509**, 108–118.
44 J. Noolandi, M. C. Peterman, P. Huie, C. Lee, M. S. Blumenkranz and H. A. Fishman, Towards a neurotransmitter-based retinal prosthesis using an inkjet printer head, *Biomed. Microdev.*, 2003, **5**, 195–199.
45 G. B. Street, *et al.*, Characetrization of polypyrrole, *J. Phys., Colloq.*, 1983, **3**, 599–606.
46 Lj. Atanasoska, K. Naoi and W. H. Smyrl, XPS studies on conducting polymers: polypyrrole films doped with perchlorate and polymeric anions, *Chem. Mater.*, 1992, **4**, 988–994.
47 G. Polzonetti, *et al.*, Self-assembling peptides: a joint XPS and NEXAFS investigation on the structure of two dipeptides studied as models, *Mater. Sci. Eng., C*, 2008, **28**, 309–315.
48 T. A. Skotheim, M. I. Florit, A. Melo and W. E. O' Grady, Ultrahigh-vacuum *in situ* electrochemistry with solid polymer electrolyte and x-ray photoelectron spectroscopy studies of polypyrrole, *Phys. Rev. B: Condens. Matter Mater. Phys.*, 1984, **30**, 4846–4849.
49 T. A. Skotheim, M. I. Florit, A. Melo and W. E. O' Grady, Ultra high vacuum electrochemistry with conducting polymers, *Mol. Cryst. Liq. Cryst.*, 1985, **121**, 291–295.
50 S. Suezer, O. Birer, U. A. Sevil and O. Guven, XPS investigations on conducting polymers, *Tr. J. of Chem.*, 1998, **22**, 59–65.
51 F. Li, *et al.*, Mobility of fluorescently labeled polymer micelles in living cells, *Soft Matter*, 2011, **7**, 1214–1218.
52 J. Fitter, *et al.*, Single molecule fluorescence spectroscopy: a tool for protein studies approaching cellular environmental conditions, *Soft Matter*, 2011, **7**, 1254–1259.
53 M. R. Nabid and A. A. Entezami, A novel method for synthesis of water-soluble polypyrrole with horseradish peroxidase enzyme, *J. Appl. Polym. Sci.*, 2004, **94**, 254–258.